Vol. 12(1), pp. 12-23, July-December 2020
DOI: 10.5897/JETR2020.0691
Article Number: BD8858E64487
ISSN: 2006-9790

http://www.academicjournals.org/JETR

Journal of Engineering and Technology Research

Full Length Research Paper

Modeling and experimental validation of drying processus of the microalgue Spirulina with consideration deformation and flow mass

E. Salmwendé Tiendrebeogo[1,2,3*], G. Christian Tubreoumya[1], A. Oumar Dissa[1], A. Compaoré[1], J. Koulidiati[1], F. Cherblanc[2], A. Bere[1] and I. Youm[3]

[1]Laboratoire de Physique et de Chimie de l'Environnement (LPCE), Université Joseph KI - ZERBO, 03 BP 7021 Ouagadougou 03, Burkina Faso.
[2]Laboratoire de Mécanique et Génie Civil (LMGC), CNRS, Université de Montpellier 2, Place Eugène Bataillon 34000 Montpellier, France.
[3]Centre de Recherche sur les Energies Renouvelables (CERER), Université Cheick Anta Diop, Dakar, Sénégal.

Recieved 21 April, 2020 ; Accepted 15 June, 2020

The profiles of the material transfer properties in porous products such as Spirulina platensis during drying which characterize their behavior are often determined from different experimental points by destruction of the samples. However, for a long drying time, it's impossible to slice or cut the sample correctly because of its mechanical strength and friability. It influences the evaluation of product in cylindrical form properties during all periods of drying. The study aim to propose a model to determine the evolution of water parameters of the micro-alga Spirulina platensis during an isothermal drying. A diffusive model taking into account the deformation and the mass flow of the product is proposed. The digital resolution and the experimental measurements over a period of 120 h of drying have shown a variation of water content (kg_w/kg_{dm}) of the order of 3.12 at 0.41 in the opposite direction of the product thickness and of flow ($kg_w/m^2.s$) in the order of 9.26 10^{-10} at 2.63 10^{-8}. The proposed model satisfactorily validates the experimental drying kinetics over all drying periods and the water content profiles for thicknesses less than 10 mm. The value of R^2 obtained is of the order of 0.980, indicating a good correlation between the experimental and predicted data; whereas the root mean square error is around 0.013, showing a very good match between experimental and modeled kinetics.

Key words: Modeling, experience, drying processus, properties evolution, microalgue spirulina, deformation.

INTRODUCTION

Local mass transfers in highly porous products such as spirulina platensis during drying translate or characterize elementary movements or behaviors that the mechanic wishes to represent and predict. It is therefore important

*Corresponding author. E-mail: tiendrebeogoeloi@yahoo.fr. Tel : (+226) 50 30 70 64/65.

to know how to understand them, interpret them, measure them and compare them. Experimental studies (Kieu et al., 2018; Dissa et al., 2014; Desmorieux et al., 2010) had already defined the first tracks on mechanical behavior and water properties. In porous media, some authors consider a transfer only in the liquid phase, while others differentiate free water from bound water and take into account the transport of matter in the gas phase (Ramirez-Martinez et al., 2013; Pinto and Tobinaga, 2006; Katekawa and Silva (2006). The diffusive term is classically expressed as a function of the gradient of water content or of the concentration governed by the Fick model, but it is sometimes described by Darcy's law which allows to consider the pressure gradient. It can also be a function of the temperature gradient and take into account the mechanical properties of the product such as the Young's modulus and the fish coefficient. If mass diffusion takes place only in the liquid phase within the product, the evaporation of water takes place only on the surface. The coexistence of these phases within the material cannot be excluded. The adsorption isotherm (Monsurat et al., 2019) and the drying kinetics provide information on the overall behavior of the food dough (Tiendrebeogo et al., 2019; NFX15-119, 1999; Kalika and Alam 2014). However, it is shown in these works that the mass flux is associated with the apparent density gradients of water. These variables were identified through profiles measured experimentally by the destructive method of samples (slicing). The profiles are reconstituted from various points of experimental measurements, whereas for a very long drying time it is impossible to slice or cut the sample correctly because of its mechanical strength and its friability. This does not allow us to know the evolution of the kinetic and water parameters during all the drying periods. The experimental procedure being complex, relatively long in the slicing limit of the material and validates only part of the drying process, a prediction of the evolution of the water content profiles by a diffusion model is essential to describe the water diffusion mechanism. It is in this context that the objective of this work was to estimate the evolution of the water parameters of the *Spirulina platensis* in space and time during an isothermal drying experimentally and by a model. It's about:

(i) to model taking into account the deformation and the mass flow;
(ii) to determine the mass flow and water content fields in *S. platensis* and their evolution in space and time;
(iii) experimentally validate the modeling results.

MATERIALS AND METHODS

Experimental procedure

Sampling

The material used in this study for the validation of the mathematical model is a sample *of S. platensis* from the exploitation site located in La Fon del Cardaire, a farm located in Gignac in the south of France. A pretreatment was carried out on the harvested biomass to eliminate a good part of the culture water until reaching a given water content. Thus, the water content is reduced to 3.12 kg_w/kg_{dm} by wringing under the action of vacuum. This water content obtained after pretreatment is considered to be the initial water content of the sample for the experiment. The initial characteristic parameters recorded in Table 1 had already been determined using standard methods (NFX15-119, 1999; Tiendrebeogo et al., 2015). After spinning, the fresh *S. platensis* is transformed into samples suitable for testing. A cylindrical shape commonly used in farms during drying is adopted. A design process is defined in order to avoid the variability of the samples: the fresh biomass is molded in a cylindrical form 20 mm in diameter and 40 mm thick using a piston extruder consisting of a cylindrical tube Teflon and a steel piston; the cylindrical lateral surfaces of the samples are wrapped with a plastic film of negligible mass to avoid adhesion between the sample and the support and to ensure one-dimensional transfer; samples with initial masses on the order of 13 g are selected for use during the experiments (Figure 1). It is assumed that these conditions are met and the samples are uniform in the initial state.

To understand experimentally the distribution of water in the product during drying, the study followed the variation of the water content in the product by cutting samples. The water content in a sample slice is determined by considering the mass of this slice at a given time and that of the solid phase according to the following Equation 1:

$$w = \frac{m(x,t) - m_s}{m_s} \quad (1)$$

Drying experiments

Cutting method: samples are put to dry in a desiccator whose temperature is regulated in the order of 50°C and de *HR* is 6% respectively by a brand oven Memmert UFP 600 (Figure 2) and a potassium hydroxide solution (KOH). At each instant t, one of the samples is taken and weighed with a precision electronic balance 10^{-3}. Then it was placed it in the cutting system (Figure 3) to transform it into slices 2 mm thick perpendicular to the axis $(\vec{ox})$ using a blade 0.25 mm. The slices are then placed in the oven maintained at 70°C for 48 h to obtain their dry mass. The average water content of a sample at a given time is obtained by calculating the average of the water contents of the wafers.

In order for the moisture content profiles sought to be characteristic of a given single sample, all the samples should be in the same state at the start of the process. Thus, they are prepared under the same conditions as indicated above. The material being symmetrical, the averages of water contents of the points symmetrical compared to the median plane are considered. This approach provides access to the water content profiles $w(x,t)$ corresponding to moments of drying. Since the study aimed to characterize the phenomena of water transport in a single sample from measurements obtained on various samples, it is essential to have the same initial conditions in all the samples. Even if particular attention is paid to the preparation of samples, this methodology may present some deviations. For this, the experimental water content profiles are approached by simple polynomial equations (Equation 2) introducing 3 constant parameters a, b and c at each time.

$$w(x,t) = ax^4 + bx^2 + c \quad (2)$$

Table 1. Initial characteristics of the material. (Salmwendé et al., 2015)

Parameter	Symbol and units	Sample
Solid apparent density	ρ_s [kg/m^3]	255
Water apparent density	ρ_w [kg/m^3]	799
Solid real density	ρ_s^* [kg/m^3]	1270
Ratio of real densities	α […/…]	0.787
Porosity	ϕ […/…]	0.799
Water content	w [kgw/kgdm]	3.120

Source: Tiendrebeogo et al. (2015).

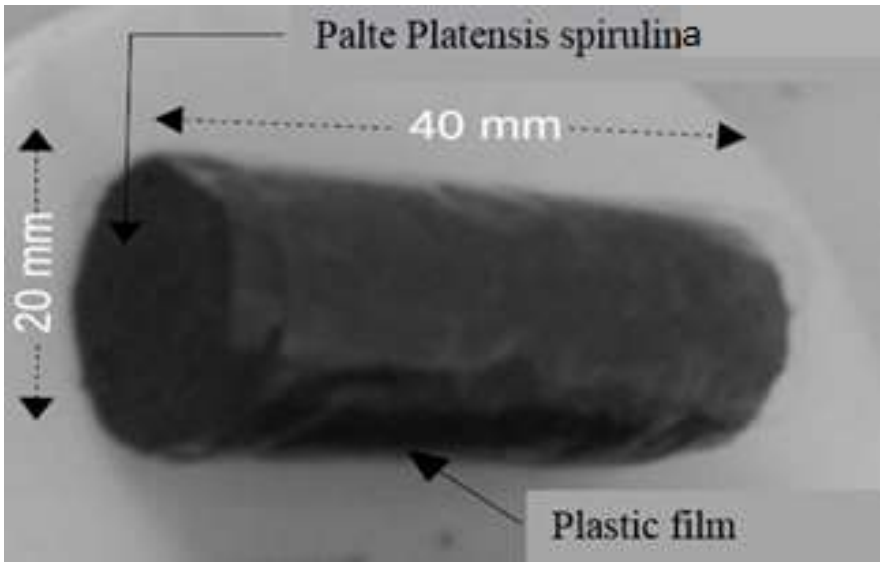

Figure 1. Study sample cylinder

Figure 2. Isothermal drying device.

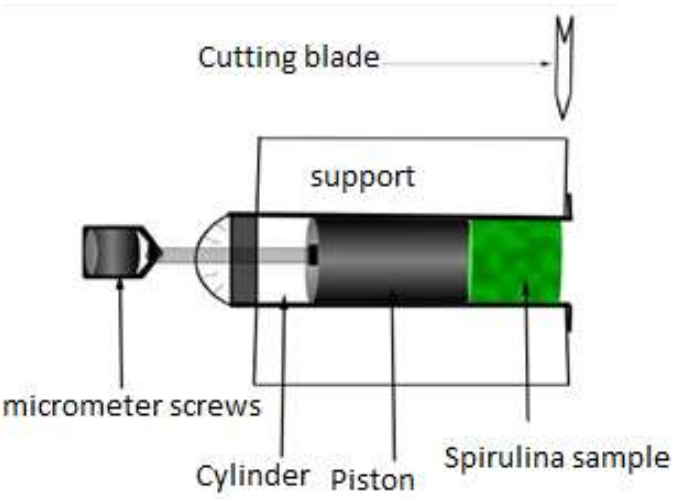

Figure 3. Device for cutting samples.

The tests were carried out at 50°C and lasted no more than 120 h (5 days). Because for a long drying period the material begins to stiffen and the cutting becomes delicate. For low temperatures (below 25°C) drying is very slow to reach values with low water content and the range of water content studied is too narrow. For too prolonged drying the material begins to denature and the development of microorganisms is observed. This could alter the water transport processes and should be avoided. Furthermore, the accuracy in the determination of experimental results estimated the statistical parameters: the coefficient R^2 and the root mean square error (RMSE). These parameters were expressed according to the following equations (Monsurat et al., 2019) which were solved by multi-linear regression analysis.

$$RMSE = \sqrt{\frac{\sum_{z=1}^{N}(Y_{\exp,z} - Y_{pre,z})^2}{\sum_{z=1}^{N}(\bar{Y}_{\exp,z} - Y_{pre,z})^2}} \quad (3)$$

$$R^2 = 1 - \frac{\sum_{z=1}^{N}(Y_{\exp,z} - Y_{pre,z})^2}{\sum_{z=1}^{N}(\bar{Y}_{\exp,z} - Y_{pre,z})^2} \quad (4)$$

MODELING

Physical configuration of model and Hypothesis

Concerning the numerical simulation, the drying conditions are the same as those of the experiment, the only difference is that one takes into account the axisymmetric geometry. That is to say the existing symmetry along the cylindrical axis ($\overrightarrow{ox}$) and the one following the median plane (the axis $\overrightarrow{oy}$) are considered (Figure 4). The simulation is done in a 2D rectangular geometry which considers only a quarter of the sample (Figure 5). The surfaces 4 and 1 respectively represent the planes of symmetries along x and y where the mass and heat fluxes are zero, as well as the surface 2 isolated with a plastic film. The surface 3 is supplied by a convective heat flow, heat flow by evaporation and an imposed mass flow which only crosses the exchange face (surface 3). The mass flow is absorbed by the air on this surface. The surface forces which could be added by the action of the film layer are negligible. For to be near to the characteristic aspects of the environment to be studied, simplifying theoretical hypotheses have been posed:

(i) the solid and liquid phases are assumed to be incompressible and the actual volume densities $\rho_w^* = cste$; $\rho_s^* = cste$ are constant.
(ii) the constitutive medium remains two-phase and modeled by a poro-elastic material.
(iii) material modeling is axisymmetric

Mass transfer equations

(i) Behavioral relationship

The filtration behavior of all fluids (liquid, vapor and gaseous) in the medium is written using the generalized DARCY law:

$$\vec{q}_{w/s} = -\frac{\bar{k}}{\mu_w}\vec{\nabla}P_w^* \quad (5)$$

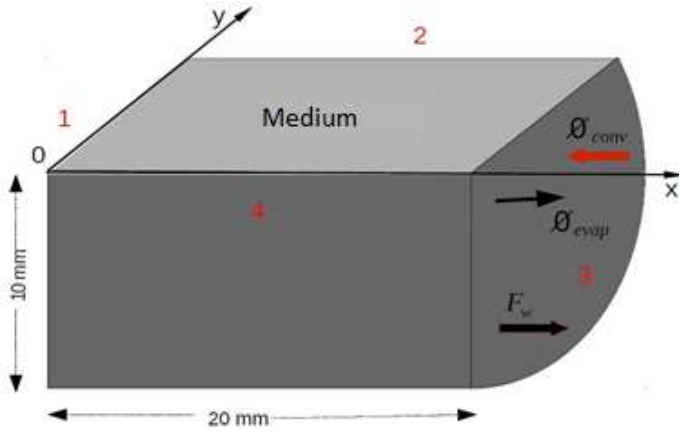

Figure 4. Quarter geometry of the sample considered for the simulation ($\varnothing_{conv}$ convective heat flow; $\varnothing_{evap}$ evaporative heat).

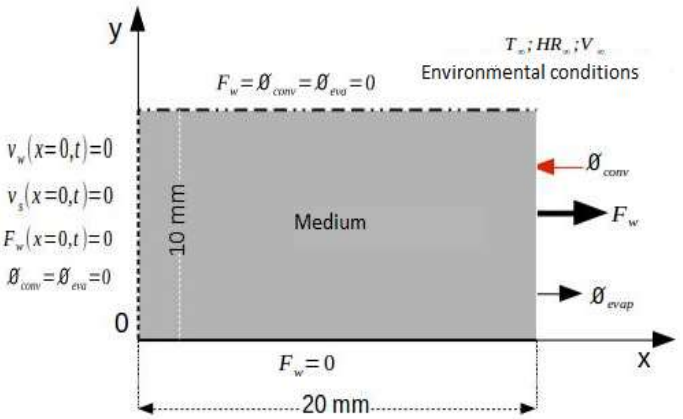

Figure 5. 2D schema of the drying conditions applied to the environment for the simulation.

The behavior of a poro-elastic material is considered:

$$\sigma_s = E\varepsilon - P_w^*\bar{\delta} \quad (6)$$

(i) Conservation equations

The formulation of the conservation equations is based on the various theoretical and experimental works developed for porous deformable and undeformable materials. For two-phase models, there is an equation for each phase (Equations 7 and 8). The liquid mass balance and solid balance equations are given respectively by Equations 3 and 4 (Anoua et al., 2014; Gowen et al., 2008).

$$\frac{\partial \rho_w}{\partial t} + \frac{\partial \rho_w u_w}{\partial x} = 0 \quad (7)$$

$$\frac{\partial \rho_s}{\partial t} + \frac{\partial \rho_s u_s}{\partial x} = 0 \quad (8)$$

The consolidation approach of an isotropic medium in linear

elasticity, developed by Marcelin Biot in 1941 was used (Seyied et al., 2015). The state parameters involved are: σ_s, ε, P_w^*. The generalized mass balance equation is given by:

$$\frac{1}{M}\frac{dP_w^*}{dt} + b\vec{\nabla}.\overrightarrow{u_s^*} = -\vec{\nabla}.\vec{q}_{w/s} \quad (9)$$

The sample to be studied being assimilated to an elastic two-phase medium, at equilibrium, the conservation of quantity is materialized:

$$\vec{\nabla}\sigma_s + b\vec{\nabla}P_w^* + \rho\vec{g} = \vec{0} \quad (10)$$

By taking Terzaghi's hypothesis (the real densities of the constituents remain constant), the Biot coefficient or the specific capacity is b = 1.0 and the compressibility coefficient is zero $\frac{1}{M} = 0$. For a medium supposed to be undeformable, the displacement of the solid can be considered zero. For this type of (isothermal) drying, the only nodal variables considered are: w and F_w. A number of hypothesis are made in addition to those previously identified:

(i) In the case of isothermal drying at low temperature, the pressure gradients are neglected.
(ii) There is only one motor gradient: water content.
(iii) The effect of gravity can be overlooked.
(iv) Evaporation of water takes place on the external surface of the medium.
(v) The compressibility effects of the gas are negligible.

Behavioral relations, Equations 7 and 8 becomes as follows:

$$\vec{\nabla}.(\overrightarrow{u_s^*} - \frac{\bar{k}}{\mu_w}\vec{\nabla}P_w^*) = 0 \quad (11)$$

$$\vec{\nabla}.E\varepsilon - \vec{\nabla}P_w^*\bar{\delta} = 0 \quad (12)$$

The water content conservation equation.

By defining the dry base water content as follows:

$$w = \frac{\rho_w}{\rho_s} \quad (13)$$

and replacing ρ_w in the liquid conservation equation (Equation 7), the study arrived at the equation below:

$$\rho_s\frac{\partial w}{\partial t} + \vec{\nabla}.(\rho_w^*\overrightarrow{u_w}) = 0 \quad (14)$$

The mass flow of evaporated water is defined by:

$$F_w = \rho_w(u_w - u_s) = \rho_w u_w - w\rho_s u_s = -D_w\frac{\partial\rho_w}{\partial x} \quad (15)$$

By applying the law of species conservation, it was deduced from Equation 15, the expression of the diffusive model in saturated medium (Justin et al., 2015; Dissa et al., 2014).

$$\frac{\partial\rho_w}{\partial t} - \vec{\nabla}.(D_w\vec{\nabla}.\rho_w) = 0 \quad (16)$$

D_w is the diffusion coefficient and it depends on the nature of the material but also on the hydrodynamic parameters. It is determined from experimental data and its evolution is materialized by the Equation 17 (Tiendrebeogo et al. 2015).

$$D_w = 2.7810^{-10} + 3.3310^{-12}\exp(3.12w) \quad (17)$$

Initial conditions and limits

At *t* =0, the initial conditions express the uniformity of the water content of the sample and the state of the mass flux at the exchange surface.

$$w = w_0 \text{ and } -D_w\vec{\nabla}.\rho_w\vec{n} = F_m = 0 \quad (18)$$

At a given time t, the condition at the level of the symmetry planes (median plane and plane along the cylindrical axis) and at the isolated surface of the product is the same:

$$-D_w\vec{\nabla}.\rho_w\vec{n} = F_m = 0 \quad (19)$$

The boundary condition associated with the exchange area is determined as follows:

$$-D_w\vec{\nabla}.\rho_w\vec{n} = F_m \quad (20)$$

F_m The mass flow imposes on the end (exchange surface) of the sample. It is represented by an exponential function resulting from a derivation of the approximate equation of drying kinetics, with L_m =0.02 m, half the length of the sample.

$F_m = \rho_w^*(a'b'\exp(-b't))\frac{\alpha}{(\alpha+w)^2}L_m$ with a' =1.885, b'= $5.948.10^{-6}$ and α the ratio of real densities is around 0.787.

Numerical resolution

For the resolution of the mathematical model, the LMGC90

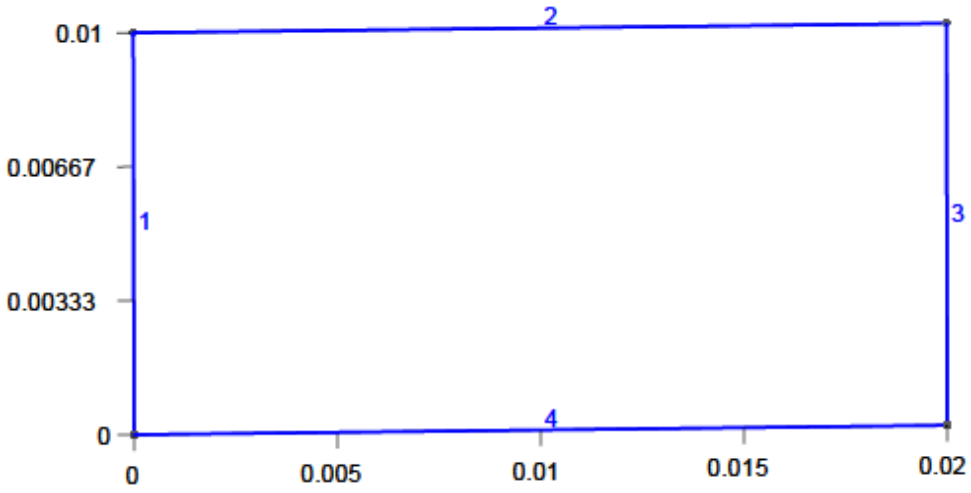

Figure 6. Sample geometry for simulation.

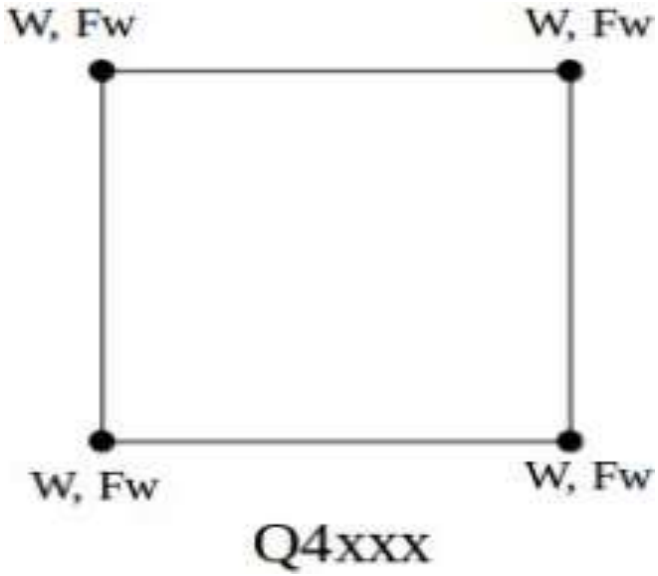

Figure 7. Mesh of elements Q4xxx.

calculation code was adopted, which takes into account all the requirements that the model requires for its numerical resolution.

Geometry of the sample

The geometric construction (Figure 6) of the sample model for the simulation is carried out in a python script defining the dimensions, shape and physical groups (end, axis, symmetry, surface).

Mesh of the model sample

Given the complexity of the model, a numerical resolution is essential and relates to the mass balance and transport equations. The method used is that of finite elements. The resolution of the finite element system amounts to meshing our material in Taylor-Hood elements (Figure 7) with well-defined nodes to carefully examine the dependence of w and the evolution of physical quantities. The problem is managed by a mesh in triangular elements (Q4xxx), order 1 with 231 nodes as shown in Figure 8.

RESULTS AND DISCUSSION

Numerical simulation

Water content and mass flux fields

Before tackling the quantitative prediction of the profile

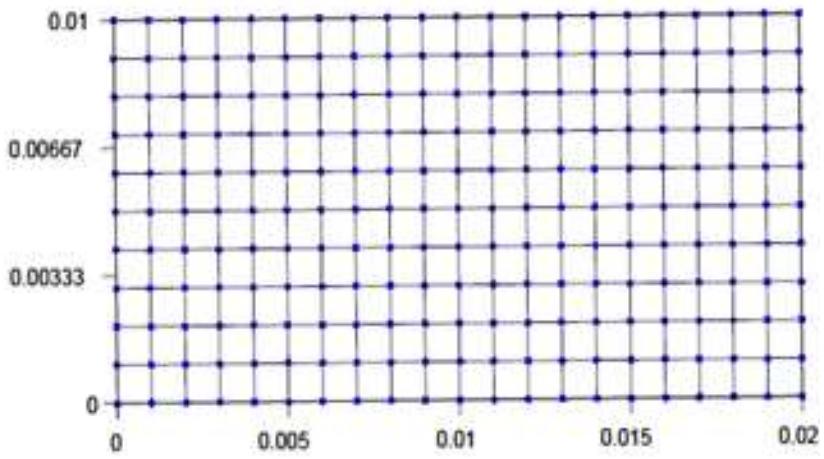

Figure 8. Sample mesh for simulation.

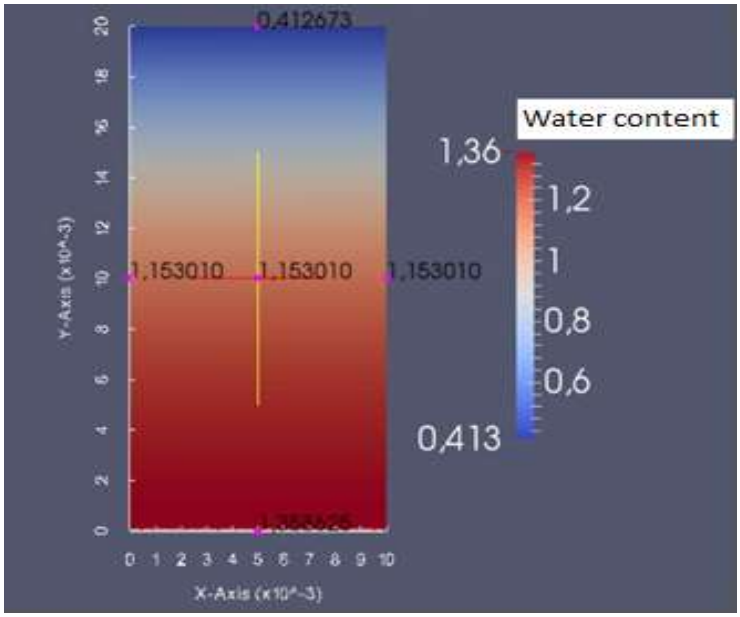

Figure 9. Simulated water content field (W_0 =3.12 kgw/kgdm).

field for different stages of exchange, it seems advisable to describe the availability of water and the evolution of mass flow during a simulation of diffusion carried out in the conditions indicated above. Figures 9 and 10 show the water content and linear density flux fields obtained after 102 h of drying a sample, respectively. In all cases, the entire sample is in the hygroscopic range with a color code expressed by the color blue for low values of quantities and the color red for high values. The analysis is based on the different colors and of course on the values taken at the reference time (120 h). Mass flows gradually settle towards the center of the product. The water content and flow in the sample vary differently, respectively on the order of 1.36 kg_w/kg_{dm} at 0.41 kg_w/kg_{dm} and in the order of 9.63 10^{-10} $kg_w/m^2.s$ at 2.2610^{-8} $kg_w/m^2.s$ This implies that the water transfer process in the product studied is governed by a single quantity: that is to say the water transport coefficient. As the drying is unidirectional, only the exchange surface dries first and has the lowest water contents. While that on the surface of symmetry, they reach 1.36 kg*w*/kg*dm*. The water content values recorded at points located on the physical groups: end, central axis, symmetry and isolated part, allow to draw only for a coast (*x)* given (thickness), the

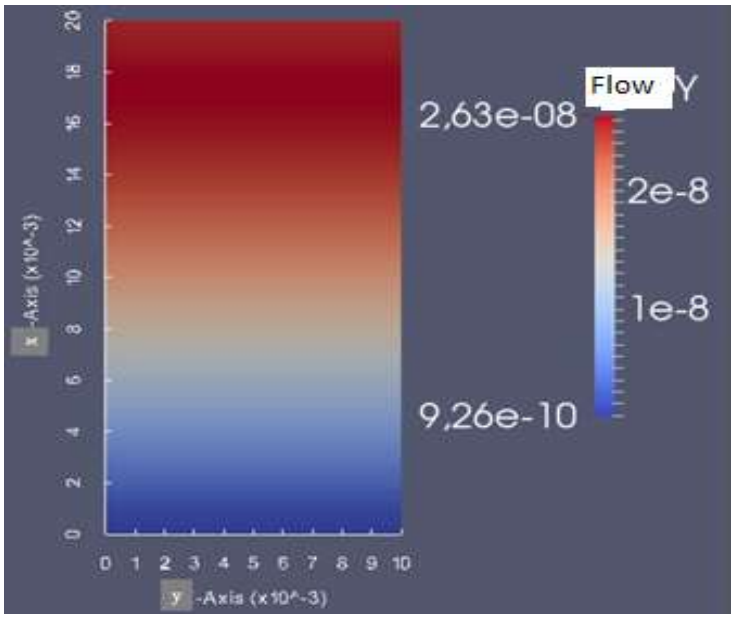

Figure 10. Champ de flux massique simulé.

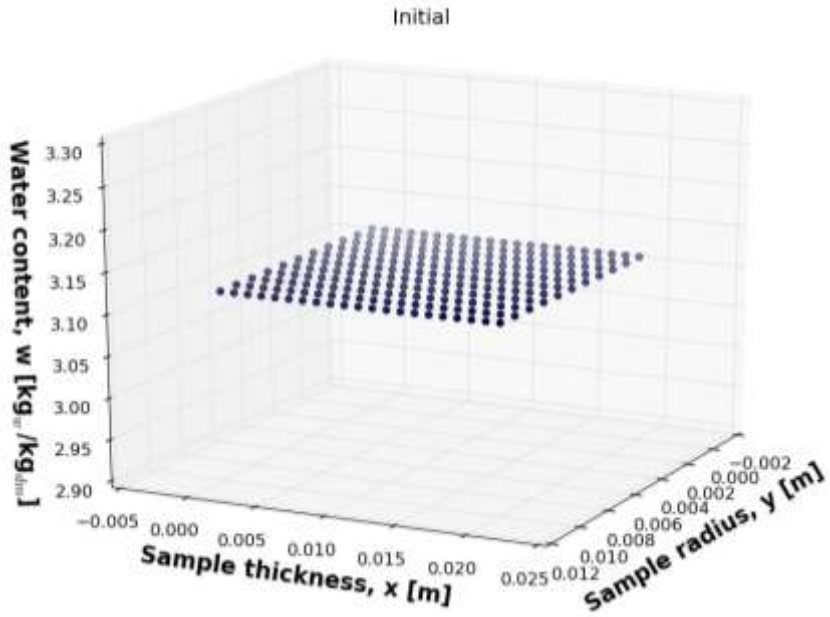

Figure 11. Fields of water content in *S. platensis* before drying (Initial state).

diffusion of water within *S. platensis* is uniform.

Evolution of spatial and temporal profiles of water content

Figures 11, 12, 13 and 14 show the spatial distribution of water within the *S. platensis* cylinder a homogeneous distribution within the product in the initial state can be clearly seen (Figure 5). From the start of the process, it becomes heterogeneous in the radial plane as well as in the axial plane and the upper surface dries faster than that of the plane of symmetry inside the product. The latter phenomenon was observed in an experimental study (Tiendrebeogo et al., 2015). Over time, the diffusion of water marks a short constant phase in the areas of the

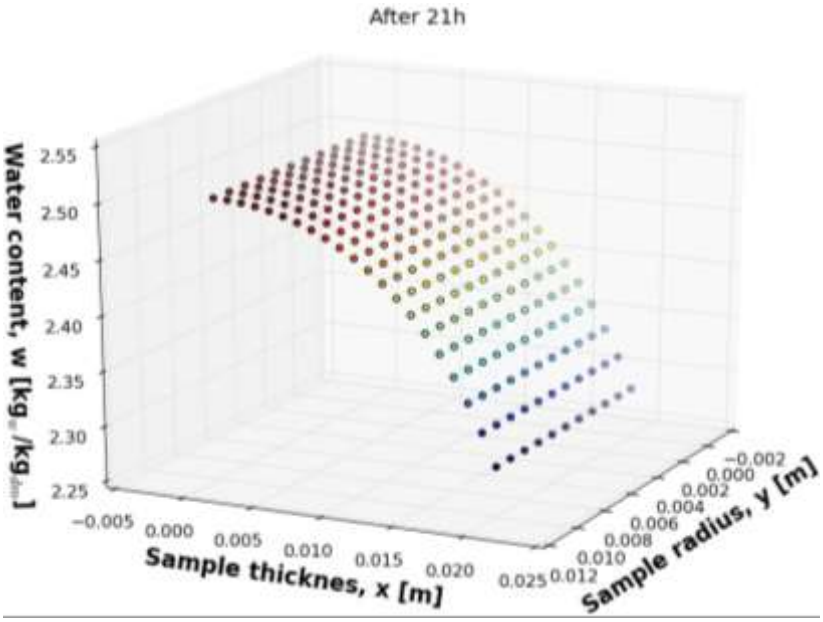

Figure 12. Fields of water content in *S. platensis* after 21 h of drying.

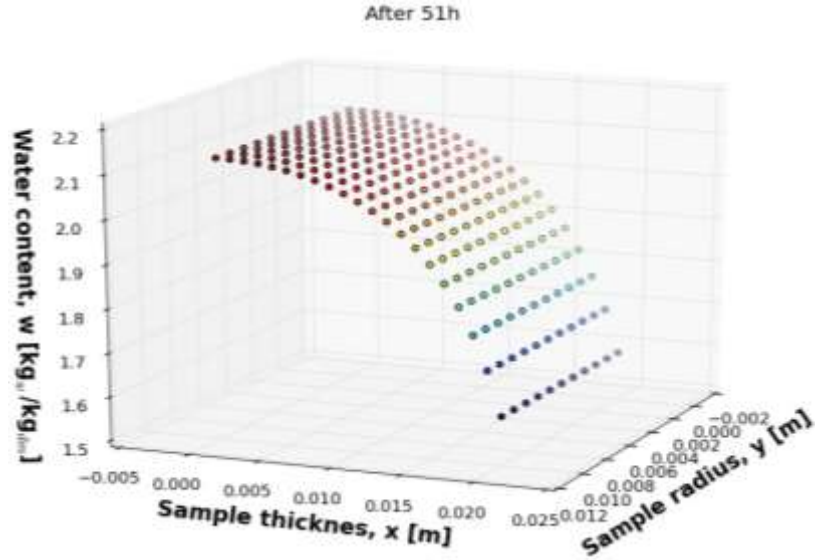

Figure 13. Fields of water content in *S. platensis* after 51 h.

sample near to its medium before going through a decreasing phase to tend towards a low water content, in this case the water content of balance. The surface exposed directly to the drying air reaches this equilibrium faster than the interior of the sample.

Experimental validation of model

The study validates the model by comparing the experimental results and those simulated. The distribution of the water content being uniform for a given thickness, the average of water content by thickness was considered to compare the results obtained by the digital method in this manuscript. The validation of the proposed model is carried out by comparing the kinetics (temporal evolution of the average water content of the product) from the numerical simulation (obtained using LMGC90) of the convective drying of Spirulina platensis, with those obtained experimentally. Indeed, this comparison shows

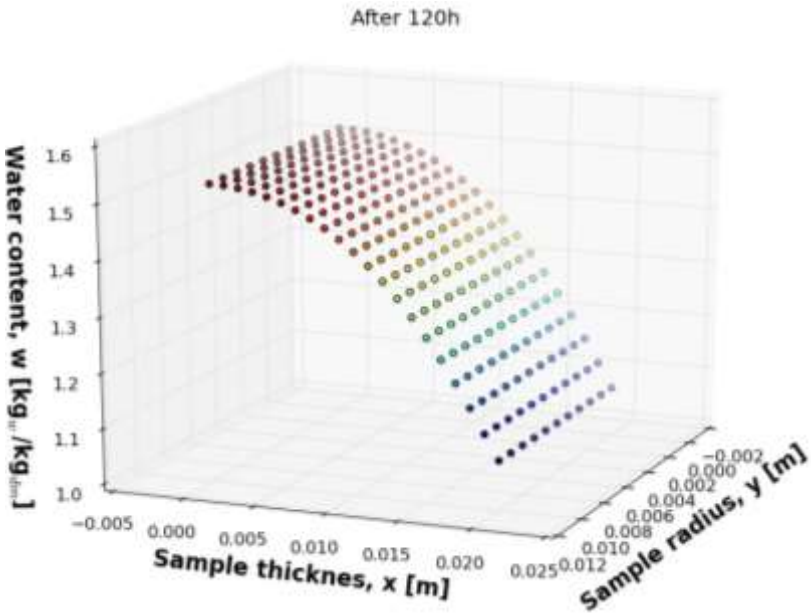

Figure 14. Water content fields in *S. platensis* at t = 120 h.

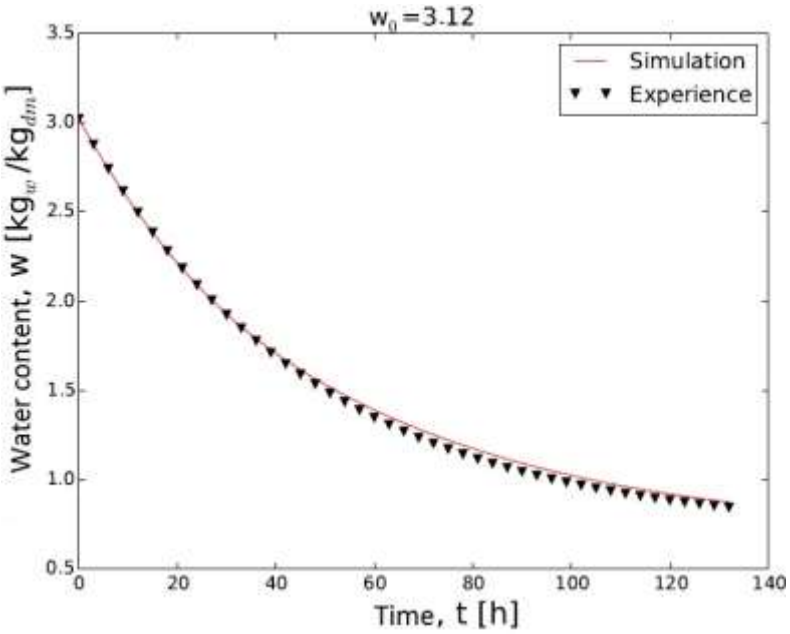

Figure 15. Comparison of simulated and experimental average water contents.

that the results of the numerical simulation are in agreement with those of the experiments (Figure 15 and Table 2). It can be observed that the proposed model is capable of predicting the drying kinetics. The differences observed between the experimental results and those obtained by the simulation can be qualified as minor. They may be due to the exact lack of knowledge of certain parameters. Another reason which can generate a gap between the experiment and the simulation, is the fact that our model concerns only a saturated medium.

Another comparison made between the experimental water content profiles and those simulated is shown in Figure 16. The simulation of the diffusion gives rise to specific curve shapes of the water content profiles and highlights the shrinkage of the solid. From the two graphs, it was noted that a concordance of the results for small thicknesses is towards the core of the material and large differences in the areas close to the exchange

Table 2. Water content and flux experimental and simulated.

	$0 \le x \le 20$		$0 \le x \le 10$		$0 \le x \le 5$	
	0 h		**120 h**		**120 h**	
	W	F_w	W	F_w	W	F_w
Experience	3.12	09.26×10^{-10}	0.70	2.63×10^{-8}	1.36	09.32×10^{-10}
Model	3.12	10.12×10^{-10}	0.80	2.05×10^{-8}	1.15	09.45×10^{-10}

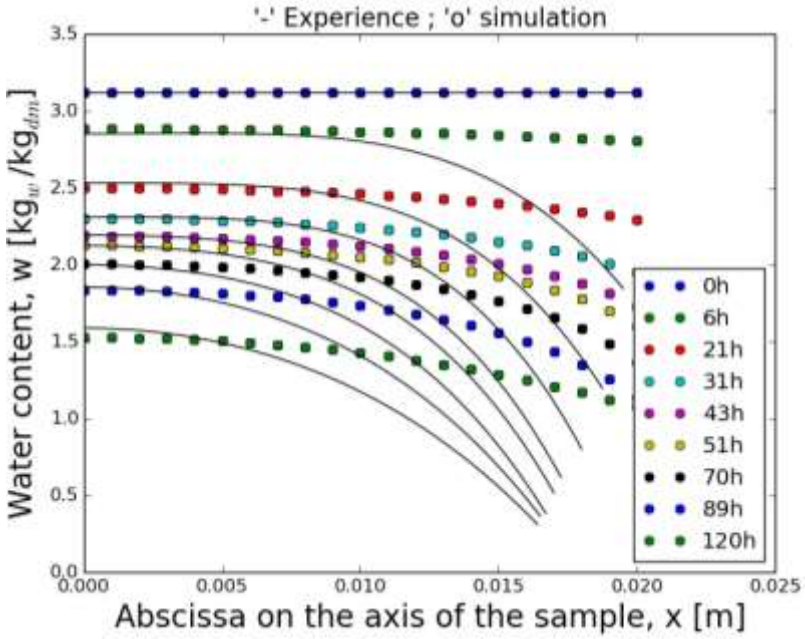

Figure 16. Comparison between the simulated profiles and those of the experience.

surface, that is to say for thicknesses greater than 10 mm. These profiles, which had been observed experimentally in 2016 (Tiendrebeogo et al., 2015), are more straightforward than those observed in coffee (Ramirez et al., 2014). The experimental results show that the contraction of the product is greater in the regions close to the surface. The fact that the shrinkage was not taken into account in the simulation could be at the origin of these observed divergences. The value of R^2 obtained is of the order of 0.980, indicating a good correlation between the experimental and predicted data; whereas the root mean square error (RMSE) is around 0.013, showing a very good match between experimental and modeled kinetics.

All the elements of comparison between simulation and experience have shown that the proposed model makes it possible to reproduce and write satisfactorily the evolution of drying kinetics throughout drying. And the water content profiles for any thickness less than 10 mm. From these results, it is observed that the range of validity of the model deteriorates at the back of the drying periods when one moves away from the core of the product, that is to say for thicknesses greater than 10 mm. Indeed, the extreme variations of the parameters of the material such as the mechanical properties (Young's modulus, Poisson's ratio) during these periods modified its mechanical behavior.

Conclusion

In this article, it was a matter of mathematically modeling and experimentally validating the evolution of the water parameters of the micro-alga *S. platensis* during isothermal drying taking into account the deformation and the mass flow. The numerical resolution of the mass transfer equations by the finite element method in the LMGC90 code made it possible to know the fields of

water content and mass flow, to represent the simulated profiles and to validate the experimental results and to define the domain of validity of the model. A model taking into account the contraction of the solid could accurately write the diffusion of water in *S. platensis*.

CONFLICT OF INTERESTS

The authors have not declared any conflict of interest.

NOMENCLATURE

HR, relative humidity (%); dm, dry matter (kg_w/kg_{dm}); d, cylinder diameter (m); w, water content (kg/kg); t, time (s); D_w, transport coefficient (m^2/s); F_w, mass water flux ($kg.m^{-2}.s^{-1}$); G_w, gradient of water density (kg/m^4); m_{eq}, equilibrium mass of sample (kg); m_i, sample initial mass (kg); x, sample thickness (m); m_s, dry mass of sample (kg); u_s, velocity of the solid phase (m/s); u_w, velocity of the liquid phase (m/s); w_{eq} equilibrium moisture content (kg/kg); α, real densities ratio (%); ρ_s, solid apparent density (kg/m^3); ρ_w, water apparent density (kg/m^3); ρ_s^*, solid real density (kg/m^3); ρ_w^*, water real density (kg/m^3); ϕ, porosity (%); R^2, coefficient of determination and RMSE, root mean square error.

REFERENCES

Anoua M, Ramirez-Martinez A, Cherblanc F, Bénet JC (2014). The use of chemical potential to describe water transfer in complex media with strong solid-liquid bonding. Transport in Porous Media 102:111-122.

Desmorieux H, Madiouli J, Herraud C, Mouaziz H (2010). Effects of size and form of Arthrospira spirulina biomass on the shrinkage and porosity during drying. Journal of Food Engineering 100 :585-595.

Dissa A, Compaore A, Tiendrebeogo E, Koulidiati J (2014). An effective moisture diffusivity model deduced from experiment and numerical solution of mass transfer equations for a shrinkable drying slab of microalgae spirulina. Drying Technology 32:1231-1244.

Tiendrebeogo ES, Dissa AO, Cherblanc F, Youm I, Bénet JC, Compaoré A, Koulidiati J (2015). Characterization of Two Different Stumps of Spirulina platensis Drying: Assessment of Water Transport Coefficient. Food and Nutrition Sciences 6:1437-144. http://dx.doi.org/10.4236/fns.2015.615148

Gowen AA, Abu-Ghannam N, Frias J, Oliveira J (2008). Modeling dehydratation and rehydratation of cooked soybeans subjected to combined microwave-hot-air drying. Innovative Food Science and Emerging Technologies 9:129-137.

Justin B, Rani PR, Jitendra P, Stefan C (2015). Drying Characteristics and Moisture Diffusivity of Distillers' Spent Grains Dried in Superheated Steam. Drying Technology 33:15-16.

Kalika G, Alam MS (2014) Mass and cool kinetics of foamed and non foamed grape concentrate during convective drying processes : A comparative study. Journal of Engineering and Technology Research 6(4):48-67.

Katekawa M, Silva M (2006). A review of drying models including shrinkage effects. Drying Technology 24(1):5-20.

Kieu HL, Neli H, Abdolreza K, Andreas B, Evangelos T (2018). Superheated steam drying of single wood particles: A characteristic drying curve model deduced from continuum model simulations and assessed by experiments, Drying Technology 36(15):1866-1881.

Monsurat B, Matthew OO, Victor NE (2019). Modeling of the adsorption isotherm of *Pleurotus ostreatus* using Guggenheim-Anderson-de Boer (GAB) equation. Journal of Engineering and Technology Research 11(4):41-46.

NFX15-119 (1999). Mesure de l'humidité de l'air-Générateurs d'air humide à solutions salines pour l'étalonnage des hygromètres. Association Française de Normalisation (AFNOR).

Pinto LAA, Tobinaga S (2006). Diffusive model with shrinkage in the thin-layer drying of fish muscles. Drying Technology 24:509-516.

Ramirez-Martinez A, Salgado-Cervantes M, Rodriguez-Jimenes G, Garcia-Alvarado M, Cherblanc F, Bénet JC (2013). Water transport in parchment and endosperm of coffee bean. Journal of Food Engineering 114:375-383.

Salmwendé ET, Alfa OD, Guy CT, Kayaba H, Fabien C (2015). Couplage des mécanismes de déshydratation et du retrait de la Spiruline platensis« Arthrospiraplatensis » lors d'un séchage isotherme. Journal de la Société Ouest-Africaine de Chimie 040:17-23.

Seyied MMT, Siroos H, Hamid RT (2015). Effects of Drying Schedules on Physical and Mechanical Properties in Paulownia Wood. Drying Technology 33:15-16.

Tiendrebeogo ES, Tubreoumya GC, Dissa AO, Compaoré A, Koulidiati J, Cherblanc F, Bénet JC, Youm I (2019). Hydric Properties Evolution of Spirulina platensis during Drying: Experimental Analysis and Modeling. Food and Nutrition Sciences 10:516-577.